Estimation of Whole-Body Average SAR in Human Models Due to Plane-Wave Exposure at Resonance Frequency

Akimasa Hirata, Osamu Fujiwara, Tomoaki Nagaoka, and Soichi Watanabe, *Members, IEEE*

***Abstract*—The present study proposes an equation for estimating whole-body average specific absorption rate (WBSAR) in human body models for plane-wave exposure at whole-body resonance frequency. The present study is important because the WBSAR takes maximal at this frequency and approaches the basic restrictions in the international guidelines/standards for human protection. Therefore, the variability of the WBSAR at this frequency has attracted a great deal of attention. First, the dominant factors influencing the resonance frequency of the human body models are investigated for plane-wave exposures. An equation for estimating the WBSAR at the resonance frequency is then proposed based on an analogy to an antenna. This equation can estimate the WBSAR with the body mass index of the human body only for a given incident power density. The uncertainty of the WBSAR estimated with the proposed equation is approximately 10%, which is mainly attributed to the electrical constants of tissue, including the inhomogeneity of the human body model. The variability of the WBSAR due to the body shape was found to be 30% for humans of the same age.**

***Index Terms*—peak value estimation, resonance frequency, whole-body average SAR, whole-body exposures**

I. Introduction

THERE has been increasing public concern about the adverse health effects of human exposure to electromagnetic (EM) waves. Based on the international guidelines/standards [1, 2], whole-body average specific absorption rate (WBSAR) is used as a metric of basic restriction for radio frequency (RF) whole-body exposure. The limit is 0.4 W/kg for occupational exposure or 0.08 W/kg for public exposure. An incident electric/magnetic field or power density, which does not produce EM absorption exceeding the above basic limit, is referred to as the reference level [1] or maximum permissible exposure (MPE) [2].

It is well known that the WBSAR is largely dependent on the frequency of the incident wave despite the same incident power density, and its peaks appear at several dozen megahertz for adults [3-10] and at one hundred and a few tens megahertz for children [4, 7, 9-10]. This peak is attributed to a standing wave over the entire body. In this research field, the frequency at which the WBSAR becomes maximal is called the "resonance frequency".

The WBSAR at the resonance frequency is comparable to the basic restriction for exposure at the reference level or MPE [7, 9-10]. To investigate the variability of the WBSAR in different human models, especially in models of children, new numeric human models with different heights and weights would be required. However, it is difficult to develop different numeric human models due to significant time and cost requirements. In order to overcome this difficulty, we clarified the main contributor influencing the WBSAR in this frequency region as the electrical constant of tissue [11].

Human height at the resonance frequency is approximately 0.4 wavelengths of RF waves in free space [4, 7, 8]. The relationship between human height and the wavelength at the resonance frequency was originally derived as a highly simplified prolate spheroid or a homogeneous block model [3-4]. Even in recent studies using anatomically based models [7, 10], this relationship was maintained. However, the rationale for the relationship has not been sufficiently clarified, while it is often explained by an analogy to a half-wave dipole [12-13].

In the present study, we first investigated the dominant factors influencing the resonance frequency of the Japanese models and their corresponding spheroids for plane-wave exposure. Next, at this frequency, we proposed an equation for estimating the WBSAR based on an analogy to a half-wave dipole. The effectiveness and uncertainty of the WBSAR estimated with the proposed equation was discussed by comparing the FDTD-calculated and estimated WBSARs in different models.

II. Computational Models and Methods

A. Models

Whole-body voxel models for a Japanese adult male and a Japanese adult female were developed by Nagaoka et al. [14]. The resolution of these models was 2 mm segmented into 51 anatomical regions. Models for children of three, five and seven years of age were developed by applying a free form deformation algorithm to the male model. In this modeling, a total of 66 body dimensions was taken into account, and then reduced with different scaling factors [15]. Manual editing was applied in order to maintain their anatomical validity. The resolution of these models was kept to 2 mm. These models are illustrated in Fig. 1. The heights and weights of these models are listed in Table I.

One of the main purposes of the present study is to investigate the relationship between human height and the wavelength at

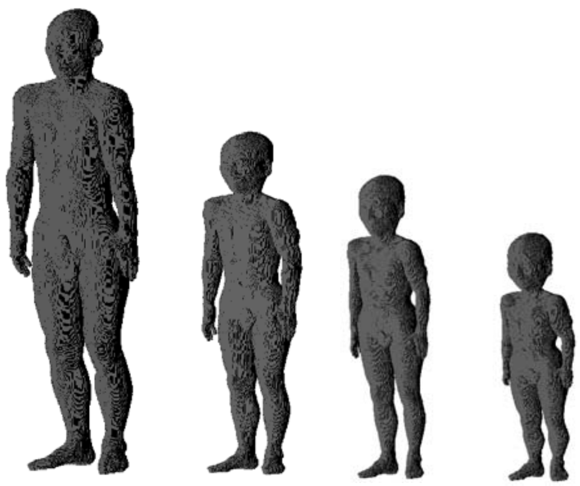

Fig. 1. Realistic body models for the Japanese model.

TABLE 1: Height and Weight of Japanese Models

	22 years	7 years	5 years	3 years
Height H [m]	1.73	1.21	1.04	0.88
Weight W [kg]	65	23	17	13

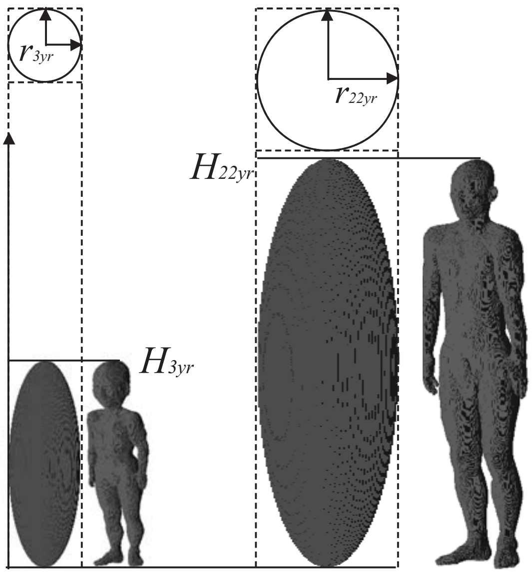

Fig. 2. Spheroids corresponding to an adult male and a three-year-old child.

the resonance frequency. Spheroids having heights coincident with those of an adult male and a three-year-old child were used in the present study (see Fig. 2). The reason for choosing spheroids is that the ratios of human body heights to the wavelengths at the resonance frequency were approximately 0.4, which is between that of a (metallic) half-wave dipole (0.48) [16] and a metallic sphere (0.33) [17].

In order to discuss the morphological difference of the human body, we also consider NORMAN, the European model, and the 10-year-old and 5-year-old child models developed from NORMAN by linear reduction [5]. The height and weight of NORMAN, 10-year-old and 5-year-old children were 1.76 m and 74 kg, 1.38 m and 33 kg, and 1.10 m and 22 kg [11], respectively. The main difference between Japanese and European child models could be anatomical reliability.

The Japanese female model HANAKO, European female model NAOMI, and the adult male model developed at Brooks Air Force Base (BAFB) are also considered. The height and weight of HANAKO were 1.61 m and 53 kg [14], those of NAOMI, and the BAFB were 1.63 m and 60 kg [8], and 1.88 m and 105 kg [18], respectively. The reason for using these models is to discuss the effect of anatomical configuration. The body mass index (BMI) for the BAFB model is 29.8, which is classified as overweight. Note that BMI is a statistical measure of the weight of a person scaled according to height [19], and its strong correlation with the percentage of body fat has been reported for a given gender and age (see adults [20] and children [21]). Other anatomically based models are generally classified as being normal with respect to weight [5, 8, 14-15].

B. Computational Methods and Conditions

The finite-difference time-domain (FDTD) method [22] was used to calculate the electromagnetic power absorbed in the human models. For geometries in which the wave-object interaction has to be considered in open regions, the computational space has to be truncated by absorbing boundaries. We adopt perfectly matched layers [22] as the absorbing boundary, because this offers the advantages of very low reflections and relatively low computational costs. We chose the thickness of the perfectly matched layer as 12 cells. The maximum conductivity of the layers was determined so that, theoretically, it has an attenuation of 40 dB for the normal incident to the layers.

Either of the models is located in free space. The separation between the human model and the 12-layered perfectly matched layers was maintained at 100 mm (50 cells). For this scenario, the effect of the absorbing boundary on the WBSAR can be neglected. The computational uncertainty in the WBSAR computation due to the absorbing boundary condition is found in [7, 23]. Our computational code has been validated through intercomparison with other studies [24].

As an incident wave, a plane wave with a vertical polarization is considered. The reason for choosing this polarization is that the WBSAR becomes maximal due to a standing wave over the human body [4]. Therefore, the WBSAR under this condition is essential [4-10] from the aspect of the relationship between basic restriction and the reference level/MPE in the safety guidelines/standards [1-2]. Note the multipath exposure has been investigated and reported to be worse for some realistic conditions in the GHz regions [24, 25]. Field/power density are intended to be spatially averaged over the body of the exposed individual. [1, 2]. Since the primary goal of the present study is to clarify the relationship between the basic restriction and the reference level/MPE, compliance assessment for such realistic exposure is beyond the scope of the present paper.

The electrical constants of tissues are taken from [26]. When considering homogeneous human/spheroid models, the electrical constants of 2/3 that of muscle were used. Note that the human body is comprised of high and low water content tissues with the ratio of 2:1. The electrical constants of low-water-content tissues, such as fat and bone, are much smaller than those of high-water-content tissues, such as muscle. Therefore, the electrical constant of 2/3 that of muscle, which is a representative of high water content tissue, is often considered for fundamental discussion.

III. Computational Results

A. Dominant Factors Influencing the Resonance Frequency

This subsection discusses dominant factors influencing the resonance frequency of human bodies. Two main factors can be considered: the shape of the model and the electrical constants of the tissue.

Figure 3 shows the relationship between the spheroid height normalized by the wavelength at the resonance frequency *H/λ* and the radius normalized by the spheroid height *r/H*. In this figure, the range of the spheroid radius, corresponding to a human body, is also shown. The boundary of this range was determined such that the weight or the surface area of the spheroid coincides with those of an adult male and a three-year-old child. Note that the surface area of the human body was derived from an empirical formula for Japanese subjects [27]. In order to discuss the effect of electrical constants, spheroids comprised of perfect conductor were also considered. The resonance frequency for the metallic models has been determined such that induced current at the mid-horizontal plane becomes maximal for plane wave incidence.

As shown in Fig. 3, *H/λ* decreases with increasing *r/H* because the longitudinal dimension becomes longer with increasing circumference of the spheroids, thereby lowering the resonance frequency. For the metallic spheroid corresponding to the adult male, *H/λ* was 0.41-0.45, and *H/λ* was 0.43-0.44 for the child. Similarly, *H/λ* was 0.38-0.45 for the dielectric spheroid of the adult, while *H/λ* was 0.41-0.43 for that of the child. These comparisons reveal that the circumference of the spheroid changes the resonance frequency by 7-15%. In addition, the effect of the electrical constant of the tissue was 0-7%, which is smaller than that due to the circumference. The resonance frequency of the dielectric spheroid coincides reasonably with an *H/λ* of 0.4, as reported in previous studies [3-4].

Next, we discussed the resonance frequency in realistic-shaped human body models, as shown in Fig. 1. The effect of the shape of the human body and the tissue inhomogeneity on the resonance frequency is then investigated. The WBSARs in the Japanese models were calculated at intervals of 5 MHz, and their resonance frequencies were estimated using a first-order linear interpolation. As shown in Table 2, *H/λ* was in the range of 0.38 and 0.40 in the anatomically based models. This range is in excellent agreement with those for the anatomic models developed at

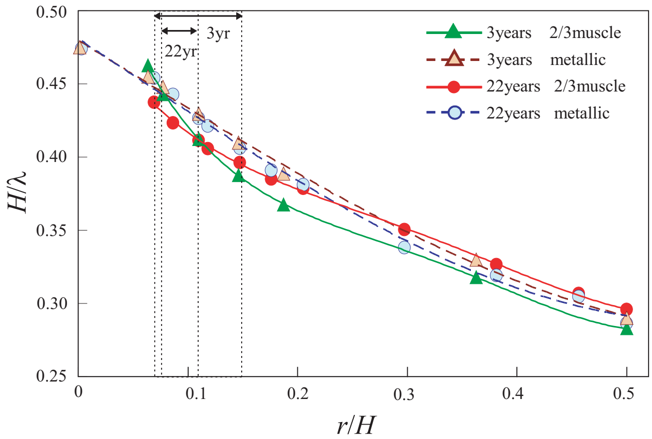

Fig. 3. Relationship between the height of the spheroid at which WBSAR takes its maximal value and the radius of the spheroid. The resonance frequency for the metallic models has been determined such that induced current at the mid-horizontal plane becomes maximal for plane wave incidence.

Table 2: Resonance Frequency in Different Human Models

	22 years	7 years	5 years	3 years
f_{res} [MHz]	65	95	115	136
H/λ	0.40	0.40	0.38	0.38

University of Florida, 0.38-0.41 [10] and NORMAN and its child models, 0.38-0.40 [11]. For HANAKO, NAOMI, and the BAFB model, *H/λ* were 0.40 (74 MHz), 0.40 (74 MHz), and 0.39 (65 MHz), respectively, suggesting that the effect of anatomy on this relationship is sufficiently small.

Values of *H/λ* of 0.38-0.40 for the realistic-shaped homogenized models were in reasonable agreement with those of the dielectric spheroids of 0.38-0.45. However, some difference was observed between these two values. As mentioned above, there are two main reasons for this difference, namely, tissue inhomogeneity and body shape. In order to investigate the effect of tissue inhomogeneity, these Japanese models were homogenized with an electrical constant of 2/3 that of muscle. From our computation, the differences in the resonance frequencies between heterogeneous and homogeneous models were less than 1%. From Fig. 3, the definition of the circumference of the human model is also thought to affect these differences, because the corresponding radius of circumference differs greatly, even among adults and children.

B. Formula of Whole-Body Average SAR at the Resonance Frequency

The main purpose of this subsection is to propose an equation to estimate the WBSAR in order to discuss the variability of the WBSAR in different human models. As shown in Section IIIA, as well as in previous studies [12-13], it is reasonable to consider the human body approximately as a half-wave dipole.

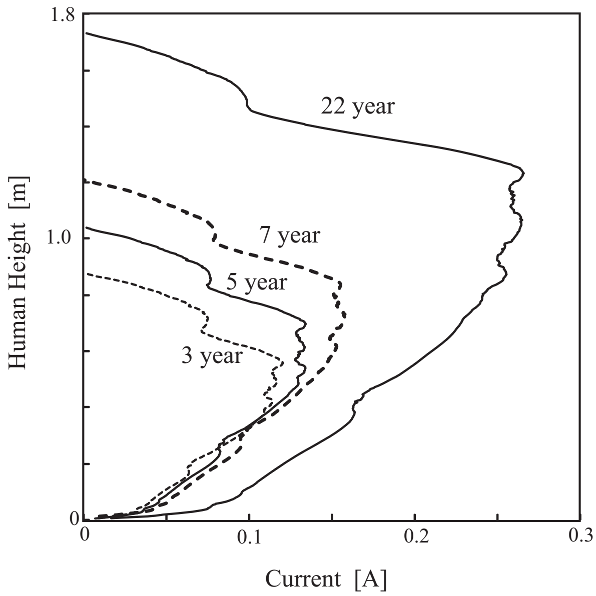

Fig. 4. Vertical conduction current in different Japanese body models at respective resonance frequencies.

The resonance frequency can be reasonably estimated from the height of the human subjects.

In order to further confirm the analogy of a half-wave dipole and human body models at their respective resonance frequency, the conduction currents along the vertical axis were calculated for the Japanese models. As shown in Fig. 4, the vertical conduction current in the human body is similar to that for the half-wave dipole [16]. The vertical conduction current was obtained by integrating FDTD-derived conduction current density along the vertical axis over each horizontal plane. As seen from Fig. 4, a number of ripples, however, were observed in the conduction current distribution. These ripples appear because the effect of the displacement current is not neglected at or above approximately 10 MHz [29]. For human exposures to frequencies below approximately 10 MHz, at which the human body becomes a good conductor, no ripples were observed [29]. The current distribution is then closer to that of the half-wave dipole. Based on this discussion, the power absorbed in the human body is expected to be smaller than that of a half-wave dipole with a matched load, because the human body does not act as a good conductor in this frequency region. Keeping this point in mind, we attempted to estimate the WBSAR in the human body models using an analogy to the half-wave dipole, despite some limitations.

Let us summarize the fundamental characteristics of the half-wave dipole antenna. For the current distribution on the antenna $I(z)$ and the maximum current I_o [A], the effective height of the antenna L_e [m] is given by the following equation [17]:

$$L_e = \frac{1}{I_0}\int_0^L I(z)dz, \tag{1}$$

where L [m] is the physical height of the antenna. The effective height of the half-wave dipole is given by the following equation [17]:

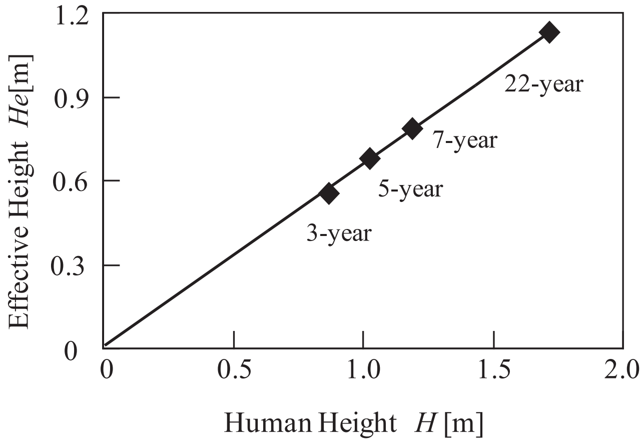

Fig. 5. Relationship between human height and effective height for different human models at respective resonance frequencies.

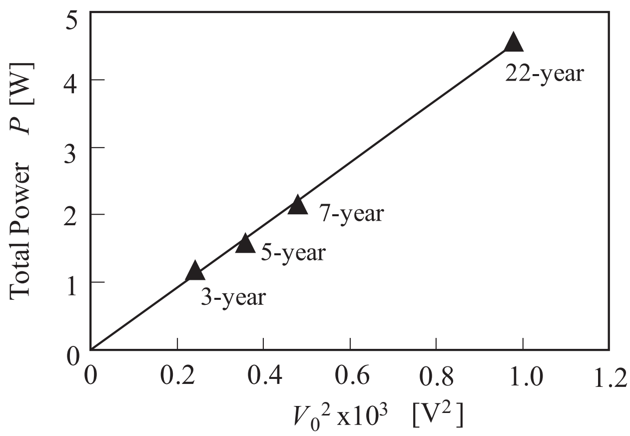

Fig. 6. Relationship between induced voltage and absorbed power in Japanese body models at respective resonance frequencies.

$$L_e = \frac{\lambda}{\pi} \cong 0.636L. \tag{2}$$

For an antenna of known effective height, the induced voltage V_o [V] is given by multiplying the effective height by the incident electric field or incident power density S_{inc} [W/m^2]:

$$V_o = \sqrt{120\pi S_{inc}}L_e. \tag{3}$$

where 120π [Ω] is an impedance of space.

From (2) and (3), we can estimate the induced voltage in the antenna.

Fig. 5 shows the relationship between the effective antenna height and the effective human height. The antenna effective height was calculated with (1) for the current distribution shown in Fig. 4. As shown in this figure, strong correlation was observed between the human height H [m] and the human effective height as an antenna H_e [m]. In the results for the Japanese models, the regression line obtained using the least squares method was represented as:

Table 3: Comparison of FDTD-Calculated and Estimated WBSARs ($\times10^{-2}$ W/kg) in (a) Japanese Male Models and (b) NORMAN (NOR) and Its Child Models (10 Years and 5 Years), BAFB Model, HANAKO (HAN), and NAOMI (NAO) at Respective Resonance Frequencies (Power Density of 2 W/m^2)

(a)

	22 years	7 years	5 years	3 years
FDTD	7.03	9.38	9.34	9.11
Estimated	6.94	9.52	9.56	8.98
Diff. [%]	1.5	2.2	1.5	1.2

(b)

	NOR	10 years	5 years	BAFB	HAN	NAO
FDTD	6.20	8.31	8.45	4.87	6.89	6.06
Estimated	6.23	8.54	8.75	5.03	7.33	6.65
Diff. [%]	0.4	2.7	3.4	3.2	6.3	9.8

$$H_e = 0.657H, \quad (4)$$

where the coefficient of determination was 0.999. From (2) and (3), the current distribution on the human body can be confirmed to be similar to a half-wave dipole.

Next, the relationship between induced voltage V_o [V] and the power absorbed in the human body was investigated in order to examine the radiation resistance [17] considering the human body as an equivalent antenna. As seen from Fig. 6, strong correlation was observed between the induced voltage and the total power P [W]. Their relationship is characterized by the least squares method using the following equation:

$$P = 4.62\times10^{-3}[S]V_o^2. \quad (5)$$

The coefficient of determination was 0.998. From the reciprocal of the coefficient in (5), the radiation resistance for the human body was approximately constant at 216 Ω, even though the resonance frequency and body shape differ for different models. From (3), (4), and (5), we can obtain an equation to estimate the WBSAR in a human body model by the following equation:

$$\begin{aligned} WBSAR &\cong 0.752 S_{inc} H^2 / W \\ &= 0.752 S_{inc} / B, \end{aligned} \quad (6)$$

where W is the weight of the human, and B (=W/H^2) [kg/m^2] is the BMI. Note that Conil et al. used BMI for discussing the variability in the WBSAR [9]. From Eq. (6), we can simply estimate the WBSAR in terms of BMI of the human body only.

C. Validity of Formula for Estimating Whole-Body Average SAR at the Resonance Frequency

In order to discuss the formula developed in the previous subsection, the WBSARs in the anatomically based model calculated by the FDTD method and estimated from (6) are listed in Table 3. In this analysis, NORMAN and its child models, the Japanese female adult model, and the BAFB model are also used for comparison. As shown in the table, the

Table 4: Comparison of FDTD-Calculated and Estimated WBSARs ($\times10^{-2}$ W/kg) in Homogenized (a) Japanese Male Models and (b) NORMAN (NOR) and Its Child Models (10 Years and 5 Years), BAFB Model, HANAKO (HAN), and NAOMI (NAO) at Respective Resonance Frequencies (Power Density of 2 W/m^2). Estimated WBSARs with (6) Are Listed in Table 3.

(a)

	22 years	7 years	5 years	3 years
FDTD	7.03	9.38	9.35	9.11
Diff. [%]	1.3	1.4	2.1	1.5

(b)

	NOR	10 years	5 years	BAFB	HAN	NAO
FDTD	6.20	8.41	8.97	5.11	7.45	6.51
Diff. [%]	0.4	1.6	2.5	1.6	1.7	2.3

differences between these values are within a few percent for Japanese model, whereas the difference becomes up to 9.8% in other models. Except for Japanese male adult and child models and NORMAN, the WBSARs estimated from (6) are larger than those of FDTD-calculated values. One reason for the differences would be model inhomogeneity, because the electrical constants of tissues are the dominant factor influencing the WBSAR in this frequency region [11]. Particularly, the subcutaneous fat in HANAKO, NAOMI, and BAFB models is thicker than that in the four Japanese models that were used to derive (6). For the child models developed from NORMAN, anatomically accuracy may not be maintained since they are developed by linear scaling without manual editing, unlike the Japanese child models. In order to evaluate the effect of the model inhomogeneity, we calculated the WBSAR in the homogenized models for all the models considered. In comparing the WBSARs between the inhomogeneous and homogeneous models, we assumed that the weights of the homogenized models are the same as those of inhomogeneous models, excluding the effect of weight. As shown in Table 4, better agreement was obtained for the homogenized models than in the original inhomogeneous model. The differences between the FDTD-calculated and estimated WBSAR in the homogenized model were less than 2.5%, suggesting that the uncertainty of the WBSAR estimated from (6) due to body shape is acceptable. The dominant factor influencing the effectiveness of (6) would be tissue inhomogeneity.

D. Uncertainty of Formula Due to Tissue Inhomogeneity and Body Fat Percentage

As shown in Section III C, the effect of tissue inhomogeneity on the WBSAR estimated from (6) may not be neglected. Thus, a question arises as to if (6) is applicable to human models with different anatomies, since (6) provides a comparable WBSAR even for obese and muscular human models with similar BMIs. However, such human models with similar BMIs are not

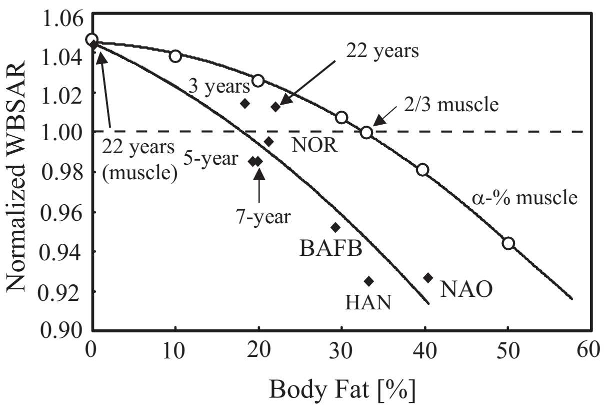

Fig. 7. Effect of body fat percentage on the WBSAR normalized by that for a homogeneous model with an electrical constant equal to 2/3 that of muscle. The curve for α-% muscle was calculated for a homogenized Japanese male adult model. The circles corresponds to the FDTD calculated WBSAR. The upper curve is derived by fitting FDTD-calculated WBSARs. The lower curve corresponds to Eq. (7).

available. This section discusses the effect of tissue inhomogeneity on the WBSAR at the resonance frequency. The body fat percentage (BFP) [32] of the model was introduced in order to facilitate the discussion for anatomically-based models. Based on recent studies, the body fat percentage for Japanese (2.5 percentile – 97.5 percentile values) has been estimated as 11-28% for 3-5-year-old child [21], 11-38% for adult males, and 17-45% for adult females [30]. We considered a Japanese adult male model in which fat was substituted into the muscle male model for empirical discussion because a muscular model of an adult male was not available.

Figure 7 shows the effect of BFP on the WBSAR of different models, together with the results for a homogeneous Japanese adult male model comprised of α-% muscle. All WBSARs in anatomically based model were normalized by those of the corresponding homogenized models with 2/3 that of muscle. In addition, α-% muscle is defined to have the electrical constants of muscle multiplied by α-%, which is similar to 2/3 muscle. In other words, α is a factor to scale the dielectric property of the homogeneous model. As shown in Fig. 7, the WBSARs in the model comprised of α-% muscle and the anatomically based models become smaller with the increase in BFP. The WBSAR in the muscular model was 3.1% larger than that in the original model and coincided well with the results for the 100-% muscle model. In particular, this figure suggests that the model homogenized as muscle could provide a conservative estimation.

For the model with the larger BFP, the WBSAR becomes smaller than that estimated with (6). The estimated WBSAR is 7-8% larger than FDTD-computed values for the models with a larger BFP (33% in HANAKO and 40% in NAOMI). Other differences may be expected for models with larger BFP. However, a discussion of such differences is not possible because no model having a larger BFP is available. In order to extrapolate the available data, regression lines approximated as a second-order polynomial are derived under the assumption that the intercept coincides with the normalized WBSAR for adult male mode, which is comprised of muscle (see Fig. 7). The coefficient of the normalized WBSAR F is given by the following equation:

$$F(p) = -4\times10^{-5}p^2 - 0.0017p + 1.044 \quad (7)$$

where p is the BFP. From (7), the uncertainty due to the body fat percentage can be roughly estimated. The limitation of this equation is the number of models considered, and so the uncertainty is estimated based on extrapolation, because muscular and obese models are not available.

E. Variability of Whole-Body Average SAR at the Resonance Frequency

The variability of the WBSAR in different humans is discussed based on Sections III C and III D. The variability of the WBSAR due to body shape can be estimated with (6). As is evident from (6), the WBSAR depends on the BMI only for the same incident power density. From (7), the uncertainty due to the BFP can be roughly estimated. From (6) and (7), the WBSAR in different humans can be estimated by the following equation:

$$WBSAR = 0.752F(p)S_{inc}H^2/W. \quad (8)$$

Note that strong correlation with the BFP and BMI has been reported for a given gender and age. (For adults and children, see [20] and [21], respectively.) The lowest WBSAR corresponds to the largest BFP and BMI, and the largest WBSAR corresponds to the smallest BFP and BMI.

Let us present the statistical body data for Japanese. The BMI roughly follows the normal distribution [19]. The mean value and standard deviation σ for Japanese can be found in [19]. The BMI changes with the age of a human during childhood. It becomes minimal at five years of age. The mean value of BMI is 15.6 for a three-year-old child, 15.2 for a five-year-old child and 16.0 for a seven-year-old child. Their standard deviation is 1.3 for three-year-old and five-year-old children and 2.0 for a seven-year-old child. For the adult male, the mean value and standard deviation are 22.7 and 3.2, respectively. For the adult female, they are 21.3 and 3.1, respectively. Let us consider the WBSAR for the range of 2 σ, in order to cover over 95% of the Japanese population. These parameters are listed in Table 5 (a). For these values, the variability of WBSAR due to the body shape is ±20-30% even for humans of the same age.

As mentioned above, the BFP for Japanese (2.5 percentile – 97.5 percentile values) was as 11-28% for 3-5-year-old children [21], 11-38% for adult males, and 17-45% for adult females [30]. Due to the lack of the data, we used the values of 3-5-year-old children for that of 7-year-old children. The coefficient F in (7) is calculated for these parameters as listed in Table 5 (b). The variability of WBSAR due to the model anatomy is 4% for the children, 8% for the adult male and 12% for the adult female.

Figure 8 illustrates the WBSAR for Japanese adults and children. In this figure, error bars are given to present the variability due to the body shape and model inhomogeneity with (8) for the parameters listed in Table 5. As seen from Fig. 8, the maximum WBSAR was observed in the five-year-old child because its BMI is the smallest. The variability of the

Table 5: (a) Mean BMI [kg/m^2] and Two Standard Deviation Below and Above Mean BMI for Adult and Child. (b)

Coefficient in (7) for Mean BFP [%] and Two Standard Deviations Below and Above Mean BFP.

(a)

	3 years	5 years	7 years	male	female
Low BMI	13.0	12.6	12.0	16.3	15.1
Mean BMI	15.6	15.2	16.0	22.7	21.3
High BMI	18.2	17.8	20.0	29.1	27.5

(b)

	3 years	5 years	7 years	male	female
Low BFP	0.965	0.965	0.965	0.921	0.887
Mean BFP	0.994	0.994	0.994	0.977	0.973
High BFP	1.020	1.020	1.020	1.020	1.000

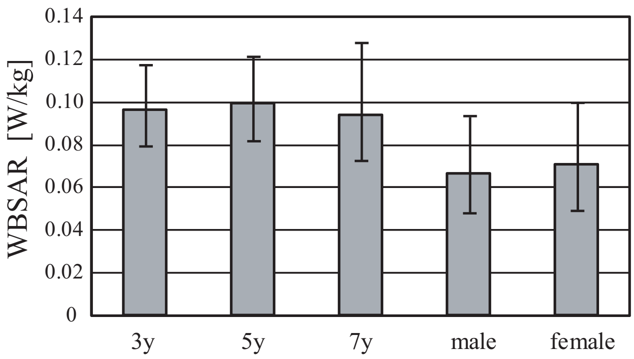

Fig. 8. Variability of WBSAR estimated with the proposed equation (2 W/m^2). Error bars represent the variability due to (8) with the uncertainty in Fig. 7 taken into account.

WBSAR due to body shape and electrical constants was found to be 30%, even for humans of the same age.

IV. Summary

The present study proposed an equation for estimating the WBSAR in human body models for plane-wave exposure at the whole-body resonance frequency. The necessity of the present study was that the WBSAR becomes maximal at that frequency and is close to the basic restriction in international guidelines/standards for human protection. Therefore, our attention was focused on the variability of the WBSAR in different human body models.

First, dominant factors influencing the resonance frequency of the human body models were investigated for plane-wave exposure. The dominant factors influencing the resonance frequency were specified as the circumference of the model and the electrical constants of tissue. Based on the discussion, H/λ was in the range between 0.38 and 0.40 in the anatomically based models.

Next, an equation for estimating the WBSAR at the resonance frequency was proposed on the basis of an analogy to an antenna. The feature of this equation was that the WBSAR can be estimated with the BMI of the human body for a given incident power density. The uncertainty of the WBSAR with the equation due to the electrical constants or model inhomogeneity was approximately 10%, as estimated from the limited number of the models. (Reply to Comment (5)) The variability of the WBSAR with the equation due to the bodily shape was found to be 30%, even for humans of the same age. In our estimation, two parameters, BMI and BFP are required. These two parameters have been reported to be close related to each other [21, 32]. Further discussion on anthropomorphic parameters is, however, beyond the scope of the present study.

From the standpoint of the safety guidelines/standards, it is essential to relate the reference level/MPE and the basic restriction, especially in developing a method to yield conservative estimate. From Fig. 7, the model with the electrical constant of muscle provided a conservative estimate. For conservative estimation, we simply replace the coefficient in (6) with 0.785, which was derived for the model comprised of muscle. When applying this value to a seven-year-old child with a BMI of 12 (2.5 percentile value), the power density required to produce the WBSAR equal to the basic restriction of 0.08 W/kg is 1.2 W/m^2. This value is smaller than the reference level /MPE in the international guidelines/standards.

When the human is grounded on a perfect conductor, the human behaves as a monopole antenna, shifting the resonance frequency [3, 4]. For such a case, the formula presented in the present study is applicable after some modification. However, the electrical constants of soil are much smaller than those of humans, and so the results do not differ greatly from the case in free space [31]. Some discussion on the WBA-SAR in the human on the perfect conductor can be found in [32].

The effectiveness of this equation for children younger than three years of age as well as other adults with different morphologies remains as future work.

Acknowledgement

This study was supported in part by the Telecom Engineering Center of Japan.

References

[1] ICNIRP (International Commission on Non-Ionizing Radiation Protection), "Guidelines for limiting exposure to time-varying electric, magnetic, and electromagnetic fields (up to 300 GHz)," *Health Phys.*, vol.74, pp. 494-522, 1998.

[2] IEEE Standard for Safety Levels with Respect to Human Exposure to Radio Frequency Electromagnetic Fields, 3 kHz to 300 GHz (C95.1), 2005.

[3] C. H. Durney, "Electromagnetic dosimetry for models of humans and animals: A review of theoretical and numerical techniques," *Proc. IEEE*, vol.68, pp.33-40, 1980.

[4] O. P. Gandhi, "State of the knowledge for electromagnetic absorbed dose in man and animals," *Proc. IEEE*, vol.68, pp.24-32, 1980.

[5] P. J. Dimbylow, "FDTD calculations of the whole-body averaged SAR in an anatomically realistic voxel model of the human body from 1 MHz to 1 GHz," *Phys. Med. Biol*., vol. 42, pp.479-490, 1997.

[6] P. J. Dimbylow, "Fine resolution calculations of SAR in the human body for frequencies up to 3 GHz," *Phys. Med. Biol.*, vol.47, pp.2835-2846, 2002.

[7] J. Wang, S. Kodera, O. Fujiwara, and S. Watanabe, "FDTD calculation of whole-body average SAR in adult and child models for frequencies from 30 MHz to 3 GHz," *Phys. Med. Biol.*, vol.51, pp.4119-4127, 2005.

[8] P. Dimbylow, "Resonance behavior of whole-body averaged specific absorption rate (SAR) in the female voxel model, NAOMI," *Phys. Med. Biol.*, vol.50, pp.4053-4063, 2005.

[9] E. Conil, A. Hadjem, F. Lacroux, M. F. Wong, and J. Wiart, "Variability analysis of SAR from 20 MHz to 2.4 GHz for different adult and child models using finite-difference time-domain", *Phys. Med. Biol.*, vol.53, pp.1511-1525, 2008.

[10] P. Dimbylow and W. Bolch, "Whole-body-averaged SAR from 50 MHz to 4 GHz in the University of Florida child voxel phantoms," *Phys. Med. Biol.*, vol. 52, pp.6639-6649, 2007.

[11] A. Hirata, S. Kodera, J. Wang, and O. Fujiwara, "Dominant factors for influencing whole-body average SAR due to far-field exposure in whole-body resonance frequency and GHz regions," *Bioelectromagnet*, vol.28, pp.484-487, 2007,"

[12] O. P. Gandhi and E. Aslan, "Human equivalent antenna for electromagnetic fields," US Patent no.5394164, Feb. 28, 1995.

[13] D. Poljak, C. Y. Tham, O. Gandhi, and A. Sarolic, "Human equivalent antenna model for transient electromagnetic radiation exposure," *IEEE Trans. Electromagnetic Compat.* Vol.45, no.1, pp.141-145, 2003.

[14] T. Nagaoka, S. Watanabe, K. Sakurai, E. Kunieda, S. Watanabe, M. Taki, and Y. Yamanaka, "Development of realistic high-resolution whole-body voxel models of Japanese adult males and females of average height and weight, and application of models to radio-frequency electromagnetic-field dosimetry," *Phys. Med. Biol.*, vol.49, pp.1-15, 2004.

[15] T. Nagaoka, E. Kunieda, and S. Watanabe, "Proportion-corrected scaled voxel models for Japanese children and their application to the numerical dosimetry of specific absorption rate for frequencies from 30 MHz to 3 GHz," *Phys. Med. Biol.*, vol.53, pp.6695-6711, 2008.

[16] J. D. Kraus and R. J. Marhefka, Antennas for all applications, 3rd Ed. McGraw-Hill, NY, 2002.

[17] J. A. Stratton, Electromagnetic Theory, Wiley-IEEE Press, 2007.

[18] P. A. Mason, W. D. Hurt, T. J. Walter, A. D'Andrea, P. Gajsek, K. L. Ryan, D.A. Nelson, K.I. Smith and J.M. Ziriax, "Effects of frequency, permittivity and voxel size on predicted specific absorption rate values in biological tissue during electromagnetic-field exposure", *IEEE Trans. Microwave Theory Tech.*, vol.48, no. 11, pp-2050-2058, 2000.

[19] A. D. Penman and W. D. Johnson, "The changing shape of the body mass index distribution curve in the population: implications for public health policy to reduce the prevalence of adult obesity," *Prev. Chronic Dis.*, vol.3, no.3, A74.

[20] A. Pietrobelli, M. S. Faith, D. B. Allison, D. Gallagher, G. Chiumello, S. B. Heymsfield, "Body mass index as a measure of adiposity among children and adolescents: a validation study," *J. Pediatr.*, vol.132, pp.204-210, 1998.

[21] S. Komiyama, T. Masuda, T. Nakao, and K. Teramoto, "The relationships between stature, fat-free mass index, and fat mass index at before and after BMI-rebound in children," *J. Health Sci.*, vol.26, pp.31-39, 2004.

[22] A. Taflove and S. Hagness, *Computational Electrodynamics: The Finite-Difference Time-Domain Method* 3rd edn (Norwood, MA: Artech House Publishers), 2003

[23] R. P. Findlay and P. J. Dimbylow, "Variations in calculated SAR with distance to the perfectly matched layer boundary for a human voxel model," *Phys. Med. Biol.*, vol.51, no.23, pp.N411-N415, 2006.

[24] G. Vermeeren, W. Joseph, C. Olivier, L. Martens, "Statistical multipath exposure of a human in a realistic electromagnetic environment," Annual Meeting of the BioElectromagnetics Society pp. 249-252, 2007.

[25] G. Neubauer, S. Cecil, P. Preiner, N. Mitrevski, G. Vermeeren, W. Joseph, L. Martens, S. Kuehn, and N. Kuster, "The relation between SAR and the electromagnetic field distribution for heterogeneous exposure conditions," Proc. European Conf. on Antennas and Propagat., 2006.

[26] C. Gabriel C, Compilation of the dielectric properties of body tissues at RF and microwave frequencies. *Brooks Air Force Technical Report* AL/OE-TR-1996 -0037, 1996.

[27] S. Fujimoto, T. Watanabe, A. Sakamoto, K. Yukawa, K. Morimoto, "Studies on the physical surface area of Japanese. 18. Calculation formulas in three stages over all ages," *Nippon Eiseigaku Zasshi*, vol.23, pp.443-50, 1968 (in Japanese).

[28] O. P. Gandhi, J.-Y. Chen, and A. Riazi, "Currents induced in a human being for plane-wave exposure conditions 0-50 MHz and for RF sealers," IEEE Trans. Biomed. Eng., vol.33, no.8, pp.757-767, 1986.

[29] A. Hirata, K. Caputa, T. W. Dawson, and M. A. Stuchly, "Dosimetry in models of child and adult for low-frequency electric fields," *IEEE Trans. Biiomed. Eng.*, vol.83, no.9, pp.1007-1012, 2001.

[30] N. Miyatake, S. Takenami, Y. Kawasaki, Y. Kunihashi, H. Nishikawa, and T. Numata, "Clinical evaluation of body fat percentage in 11,833 Japanese measured by air displacement plethysmograph," Internal Med., vol.44, no.7, pp.702-705, 2005.

[31] S. Watanabe, Y. Tanaka, M. Takahashi, M. Taki, and Y. Yamanaka, "Application of 3D-SIBC FDTD method to electromagnetic dosimetry of whole-body human models standing on non-metal ground planes," Proc. URSI Electromagnetic Theory Symposium 2004, pp.1110-1112, 2004.

[32] R. Findlay and P. J. Dimbylow, "Calculated SAR distributions in a human voxel phantom due to the reflection of electromagnetic fields from a ground plane between 65 MHz and 2 GHz," *Phys. Med. Biol.*, vol.53, no.9, pp.227-2289, 2008.